Winds from intermediate mass stars

- **Stellar and wind properties**
  - Young B, A, F type stars $\rightarrow$ negligible UV radiation field
  - Wind velocities V_*: a few 100 km s^{-1}
  - Mass loss rates $\dot{M}_* \approx 10^{-7} M_\odot$ yr^{-1}

$\rightarrow$ $\approx$ factor 10 lower than for massive stars

  - Stars are surrounded by molecular cloud gas with density $n_0 \approx 10^9$ m^{-3}
  - Flow pattern similar to winds from massive stars, but post-shock temperature for shocked wind gas is lower $T_\mathrm{S} = 10^5 - 10^6$ K $\rightarrow$ efficient cooling $\rightarrow$ one thin shell of shocked wind and swept-up IS gas

$\rightarrow$ situation similar to radiative (snowplough) phase of SNR evolution $\rightarrow$ momentum conserving, but momentum comes directly from stellar wind

  - momentum driven flow

Flow pattern around intermediate-mass stars

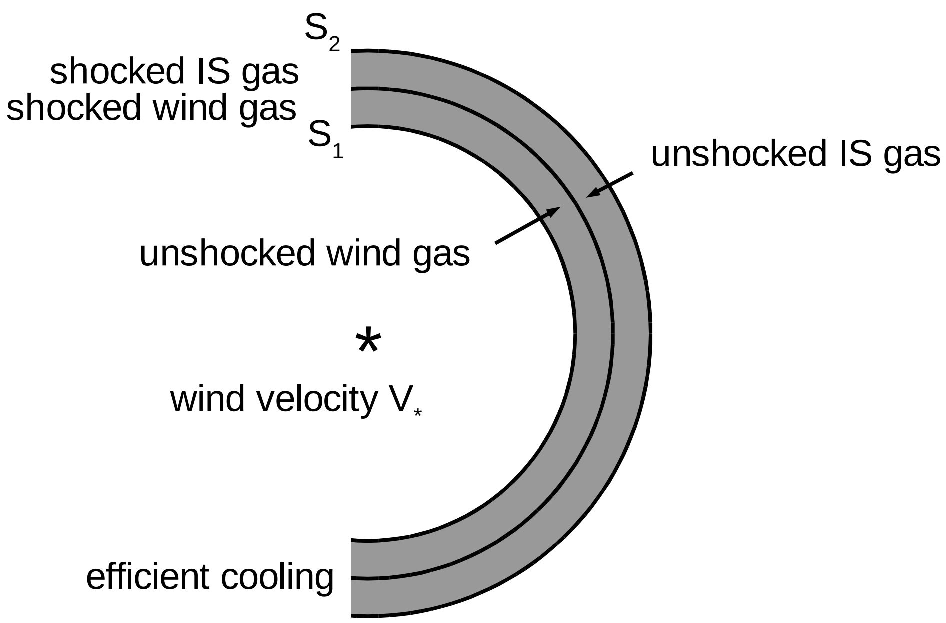

- **Expansion of the spherical shell**
  - Momentum conservation

$$\frac{\mathrm{d}}{\mathrm{d}t}(M_{\mathrm{S}}V_{\mathrm{S}}) = \dot{M}_* V_*$$

$$M_{\mathrm{S}} = \frac{4}{3}\pi R_{\mathrm{S}}^3 \cdot \mu m_{\mathrm{H}} n_0 \quad V_{\mathrm{S}} = \frac{\mathrm{d}R_{\mathrm{S}}}{\mathrm{d}t}$$

  - Integrate twice

$$R_{\mathrm{S}} = \left(\frac{3\dot{M}_* V_*}{2\pi\mu m_{\mathrm{H}} n_0}\right)^{1/4} t^{1/2}$$

  → Exponent for time dependence between that of hot star wind case and SNR momentum conserving phase
  - Efficiency for conversion of kinetic energy

$$f = \frac{M_{\mathrm{S}}V_{\mathrm{S}}^2}{\dot{M}_* V_* t} = \frac{V_{\mathrm{S}}}{V_*} = \text{ a few percent}$$

- **Non-spherical outflows from young stellar objects**
  - Most of the observed outflows are not spherical, but
    * highly collimated bipolar
    * poorly collimated bipolar
    * monopolar
  - Structures maybe produced by interaction of wind with stratified surrounding medium, e.g. an accretion disk
  - Extreme case of collimated bipolar flows: jets → conical shock wave → Herbig-Haro objects

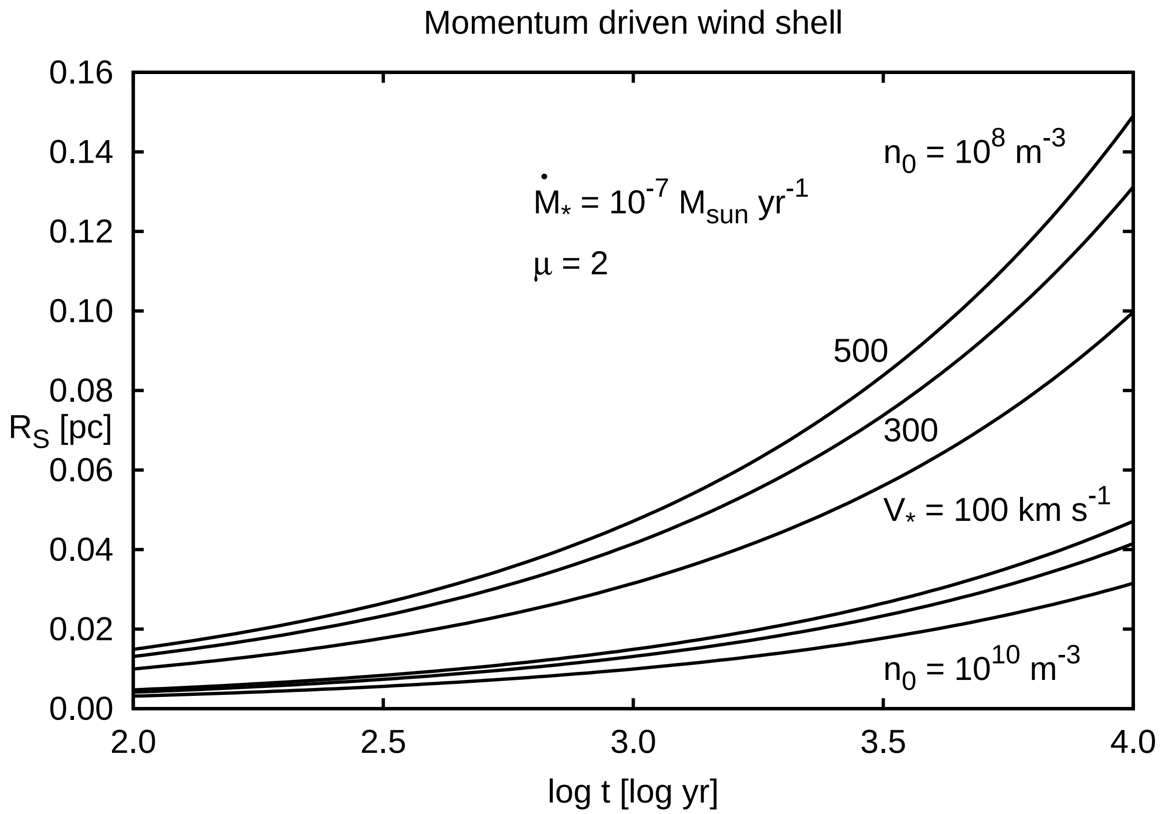
Momentum driven wind shell
0.16
0.14
0.12
0.10
0.08
0.06
0.04
0.02
0.00
R_S [pc]
2.0
2.5
3.0
3.5
4.0
log t [log yr]
$\dot{M}_* = 10^{-7}$ M_{sun} yr^{-1}
$\mu = 2$
$n_0 = 10^8$ m^{-3}
500
300
$V_* = 100$ km s^{-1}
$n_0 = 10^{10}$ m^{-3}

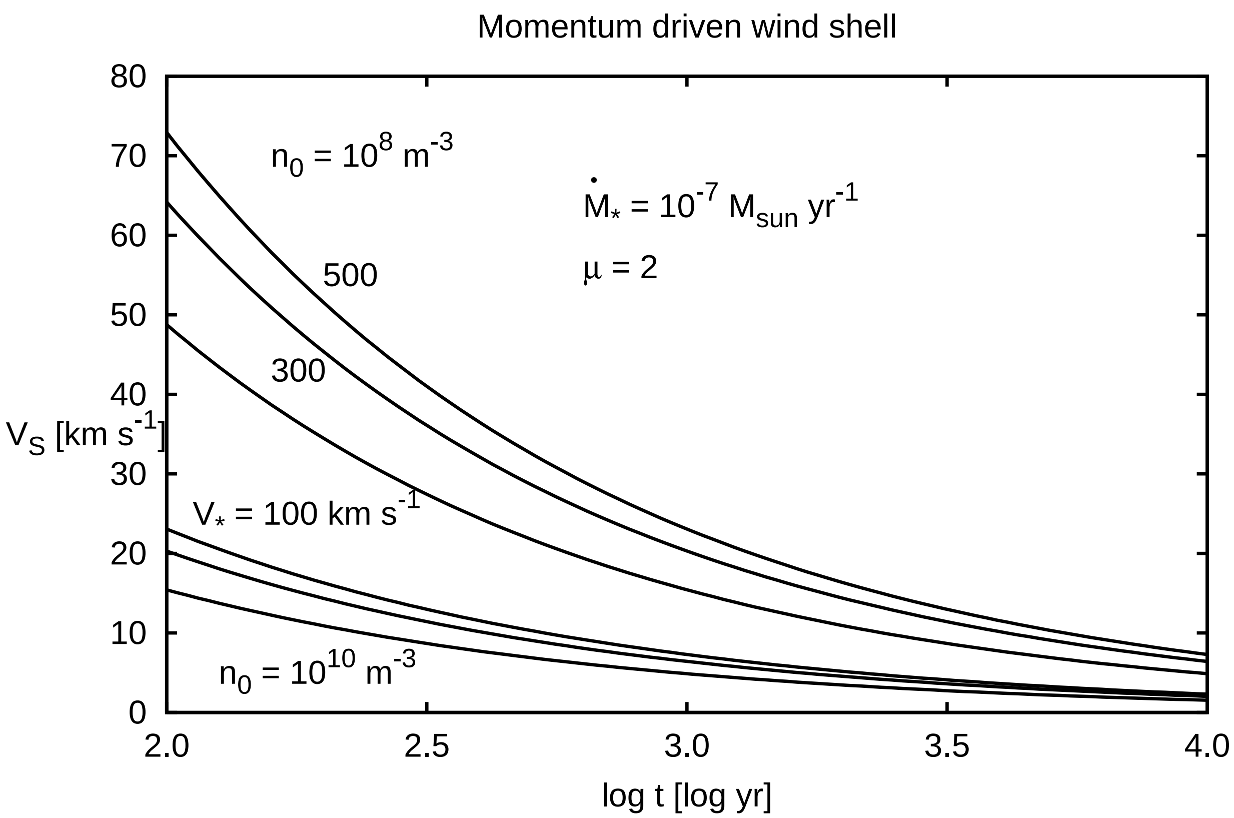
Momentum driven wind shell
80
70
60
50
40
30
20
10
0
V_S [km s^{-1}]
2.0
2.5
3.0
3.5
4.0
log t [log yr]
$n_0 = 10^8$ m^{-3}
$\dot{M}_* = 10^{-7}$ M_{sun} yr^{-1}
$\mu = 2$
500
300
$V_* = 100$ km s^{-1}
$n_0 = 10^{10}$ m^{-3}

Outflows from young stellar objects (Lada 1985)

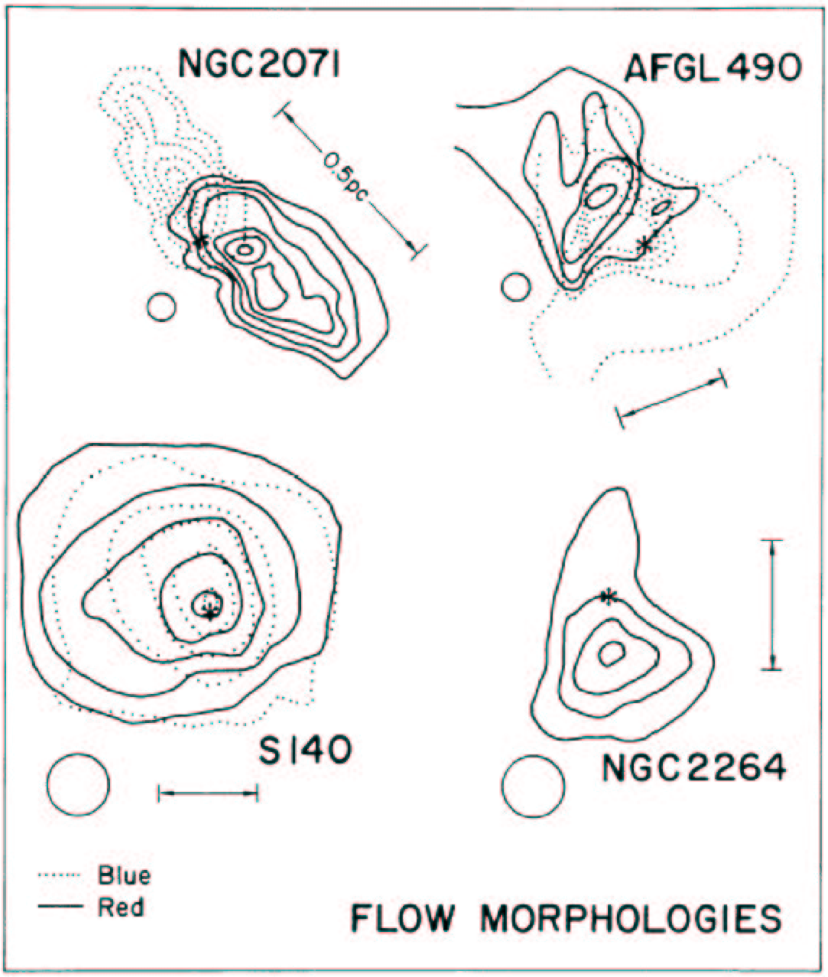

Figure 3 Maps of ^{12}CO emission from four molecular flows with differing spatial morphology. NGC 2071 is a highly collimated and bipolar hypersonic molecular flow. AFGL 490 is an example of a poorly collimated bipolar flow source, while S140 is an example of an isotropic flow source. For S140, both red and blue high-velocity emission appear to originate in the same spatial positions with no indication of a bipolar nature. NGC 2264 is an example of a monopolar source in which high-velocity molecular emission is observed on only one side (in this case, the redshifted side) of the ambient cloud emission profile.

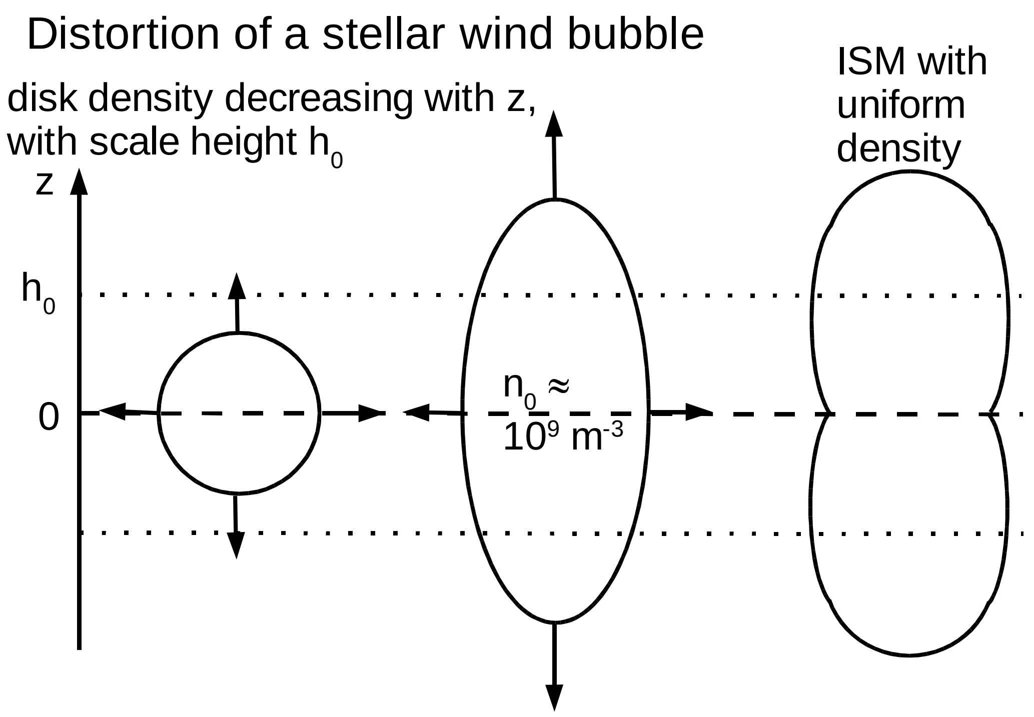

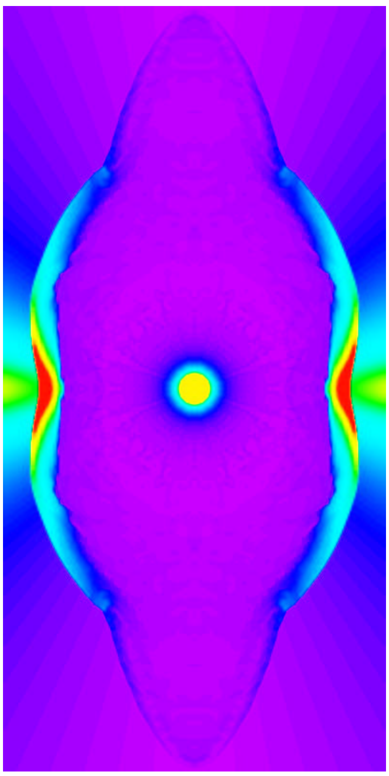

Vincent Icke (Leiden Observatory)

Numerical computation of a spherical gas stream shooting into a slightly flattened atmosphere

gas density: red ... high values
blue/purple ... low values

More simulations
of bipolar (planetary) nebulae:
http://www.strw.leidenuniv.nl/~icke/html/VincentPN.html

Free-fall collapse of a uniform cloud

- Theoretical situation to define a characteristic time for collapse of a cloud
- Spherical cloud with uniform density ρ_c
- Internal pressure neglected
- Equation of motion for shell with radius r_0 at $t = 0$

$$\frac{\mathrm{d}^2 r}{\mathrm{d}t^2} = -\frac{Gm(r_0)}{r^2} = -\frac{4\pi r_0^3 \rho_c G}{3r^2}, \quad \text{use } \frac{\mathrm{d}}{\mathrm{d}t}\left(\frac{\mathrm{d}r}{\mathrm{d}t}\right)^2 = 2\frac{\mathrm{d}r}{\mathrm{d}t}\frac{\mathrm{d}^2 r}{\mathrm{d}t^2}$$

$$\frac{1}{2}\mathrm{d}\left(\frac{\mathrm{d}r}{\mathrm{d}t}\right)^2 = -\frac{4\pi r_0^3 \rho_c G}{3}\frac{1}{r^2}\mathrm{d}r$$

$\longrightarrow$ integrate using initial conditions ($\frac{\mathrm{d}r}{\mathrm{d}t} = 0$ at $t = 0$) and take square root such that $\frac{\mathrm{d}r}{\mathrm{d}t} < 0$

$$\frac{\mathrm{d}r}{\mathrm{d}t} = -r_0\left[\frac{8\pi\rho_c G}{3}\left(\frac{r_0}{r} - 1\right)\right]^{1/2}$$

$$\frac{r}{r_0} \equiv \cos^2\theta \longrightarrow -2\cos\theta\sin\theta\frac{\mathrm{d}\theta}{\mathrm{d}t} = -\left(\frac{8\pi\rho_c G}{3}\right)^{1/2}\frac{\sin\theta}{\cos\theta}$$

$$\cos^2\theta\,\mathrm{d}\theta = \left(\frac{2\pi\rho_c G}{3}\right)^{1/2}\mathrm{d}t$$

$\longrightarrow$ integrate using initial conditions

$$t = \left(\frac{3}{8\pi\rho_c G}\right)^{1/2}\left(\theta + \frac{1}{2}\sin 2\theta\right)$$

$$r = 0 \longrightarrow \theta = \frac{\pi}{2} \longrightarrow t \equiv t_{\mathrm{ff}}$$

t_{ff} …free-fall time, in which all shells reach the cloud center

$$t_{\mathrm{ff}} = \left(\frac{3\pi}{32\rho_c G}\right)^{1/2}$$

IS cloud in hydrostatic equilibrium

- Single spherically symmetric cloud
  with radius R_c and mass M_c
- Consider forces acting on shell at radius r due to
  - external pressure P_s
  - internal pressure decreasing outwards to P_s at R_c
  - gravity
- Equilibrium:
  force due to pressure gradient equals gravitational force

$$\frac{\mathrm{d}P}{\mathrm{d}r} = -\frac{Gm}{r^2}\rho$$

$$\mathrm{d}m = 4\pi r^2 \rho \mathrm{d}r \rightarrow \frac{\mathrm{d}P}{\mathrm{d}m} = -\frac{Gm}{4\pi r^4}$$

  multiply with $4\pi r^3$ and integrate from center to surface

$$\int_0^{M_\mathrm{c}} 4\pi r^3 \frac{\mathrm{d}P}{\mathrm{d}m}\mathrm{d}m = -\int_0^{M_\mathrm{c}} \frac{Gm}{r}\mathrm{d}m$$

$$4\pi R_\mathrm{c}^3 P_\mathrm{s} - \int_0^{M_\mathrm{c}} \underbrace{12\pi r^2 \frac{\mathrm{d}r}{\mathrm{d}m}}_{1/\rho} P\mathrm{d}m = \underbrace{-\int_0^{M_\mathrm{c}} \frac{Gm}{r}\mathrm{d}m}_{E_\mathrm{g}}$$

  for a monatomic gas, $\frac{P}{\rho} = \frac{2}{3} \cdot$ internal energy per unit mass

$$\boldsymbol{4\pi R_\mathrm{c}^3 P_\mathrm{s} = 2E_\mathrm{i} + E_\mathrm{g}}$$

  E_i ... total internal energy, E_g ... gravitational energy

- Uniform cloud with density ρ_c and pressure P_c

$$E_\mathrm{i} = \frac{3}{2}\frac{P_\mathrm{c}}{\rho_\mathrm{c}}M_\mathrm{c} \qquad E_\mathrm{g} = -\frac{3}{5}\frac{GM_\mathrm{c}^2}{R_\mathrm{c}}$$

Instability of a uniform spherical cloud

- Start from equilibrium $\rightarrow$ theoretical situation
- Cloud in empty space
  - $P_{\rm s} = 0 \rightarrow 2E_{\rm i} = -E_{\rm g}$ in equilibrium
  - Investigate instability
    - * apply small periodic perturbations to density, pressure, gravitational potential and velocity
    - * for perturbed quantities, solve continuity, momentum conservation, and Poisson equations, together with an equation of state for the gas

  $\rightarrow$ "Jeans" criterion for instability
  - Criterion for collapse corresponds to $-E_{\rm g} > 2E_{\rm i}$

$$\rightarrow \frac{1}{5}\frac{GM_{\rm c}}{R_{\rm c}} > \frac{P_{\rm c}}{\rho_{\rm c}}$$

  - In terms of sound crossing time $t_{\rm c} \approx \frac{R_{\rm c}}{c_{\rm c}}$ with $c_{\rm c}^2 = \frac{P_{\rm c}}{\rho_{\rm c}}$ in isothermal cloud

$$t_{\rm c} \gtrsim \left(\frac{5R_{\rm c}^3}{GM_{\rm c}}\right)^{1/2} = \left(\frac{15}{4\pi G\rho_{\rm c}}\right)^{1/2} = \frac{2\sqrt{10}}{\pi}t_{\rm ff} \approx 2t_{\rm ff}$$

  e.g. molecular cloud ($\mu = 2$) with $n_{\rm c} = 10^9$ m^{-3} and $T_{\rm c} = 20$ K $\rightarrow t_{\rm ff} \approx 10^6$ yr, $c_{\rm c} \approx 300$ m s^{-1} $\rightarrow R_{\rm c} \gtrsim 0.7$ pc
  - In terms of cloud mass

$$M_{\rm c} \gtrsim M_{\rm crit} \propto c_{\rm c}^3 \rho_{\rm c}^{-1/2}$$

$\rightarrow$ Spontaneous star formation
  - Analysis for more realistic cloud with spherical structure gives same dependence of $M_{\rm crit}$ on T and ρ

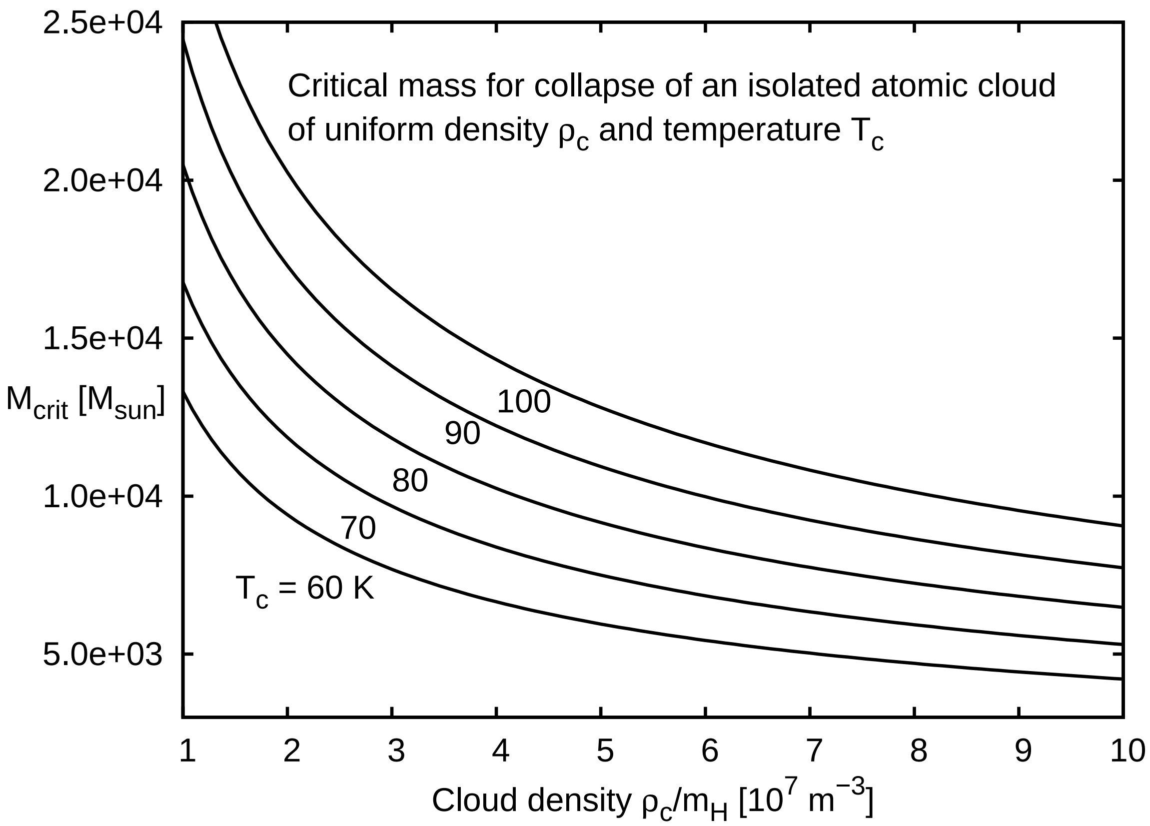

Critical mass for collapse of an isolated atomic cloud
of uniform density ρc and temperature Tc
2.5e+04
2.0e+04
1.5e+04
1.0e+04
5.0e+03
Mcrit [Msun]
100
90
80
70
Tc = 60 K
1
2
3
4
5
6
7
8
9
10
Cloud density ρc/mH [10^7 m^−3]

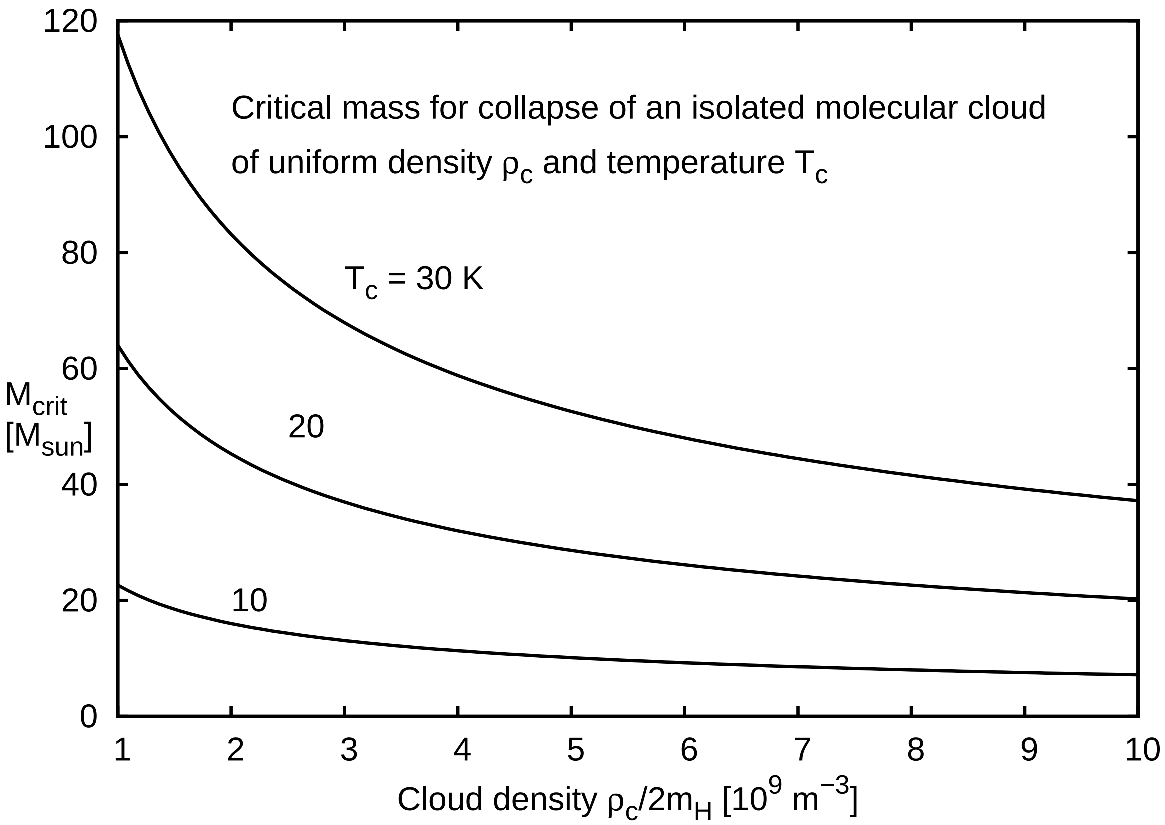

Critical mass for collapse of an isolated molecular cloud
of uniform density ρc and temperature Tc
120
100
80
60
40
20
0
Mcrit [Msun]
Tc = 30 K
20
10
1
2
3
4
5
6
7
8
9
10
Cloud density ρc/2mH [10^9 m^−3]

- Fragmentation
  - Sizes of molecular clouds are typically a few pc
    $\rightarrow$ stars are expected to form in groups within a cloud
    – supported by high binary frequency
    – e.g. $\approx$ every 2 out of 3 G stars are in binaries
  - Fragmentation within contracting part of cloud because ρ increases during collapse
    $\rightarrow M_{\rm crit}$ decreases if $c_{\rm c}$ stays constant
  - Fragmentation ends when cloud no longer isothermal, i.e. cooling by radiation becomes inefficient, and $c_{\rm c}$ increases
- Including external surface pressure
  - Equilibrium equation with $P_{\rm s} > 0$
  - For given $M_{\rm c}$ and $T_{\rm c}$
    $$P_{\rm s} = \frac{A}{R_{\rm c}^3} - \frac{B}{R_{\rm c}^4}$$
  - Maximum at $R_{\rm c} = \frac{4B}{3A}$
  - Stable regime for $R_{\rm c} > \frac{4B}{3A}$
  - $R_{\rm c}$ decreases when $P_{\rm s}$ is increased
    $\rightarrow$ can be moved into unstable regime
    $\rightarrow$ collapse $\rightarrow$ induced star formation
  - Pressure increase e.g. at ionization fronts, in shocks in stellar winds or supernova blast waves
  - For given $P_{\rm s}$ and $T_{\rm c}$ $\rightarrow$ mass-radius relationship
    $\rightarrow$ largest possible equilibrium mass
    $$M_{\rm c,max} = \left(\frac{20\pi P_{\rm s}}{G}\right)^{1/2} R_{\rm c}^2$$
    separating branches for gravitationally unstable and stable ($\rightarrow$ gravity term negligible) configurations

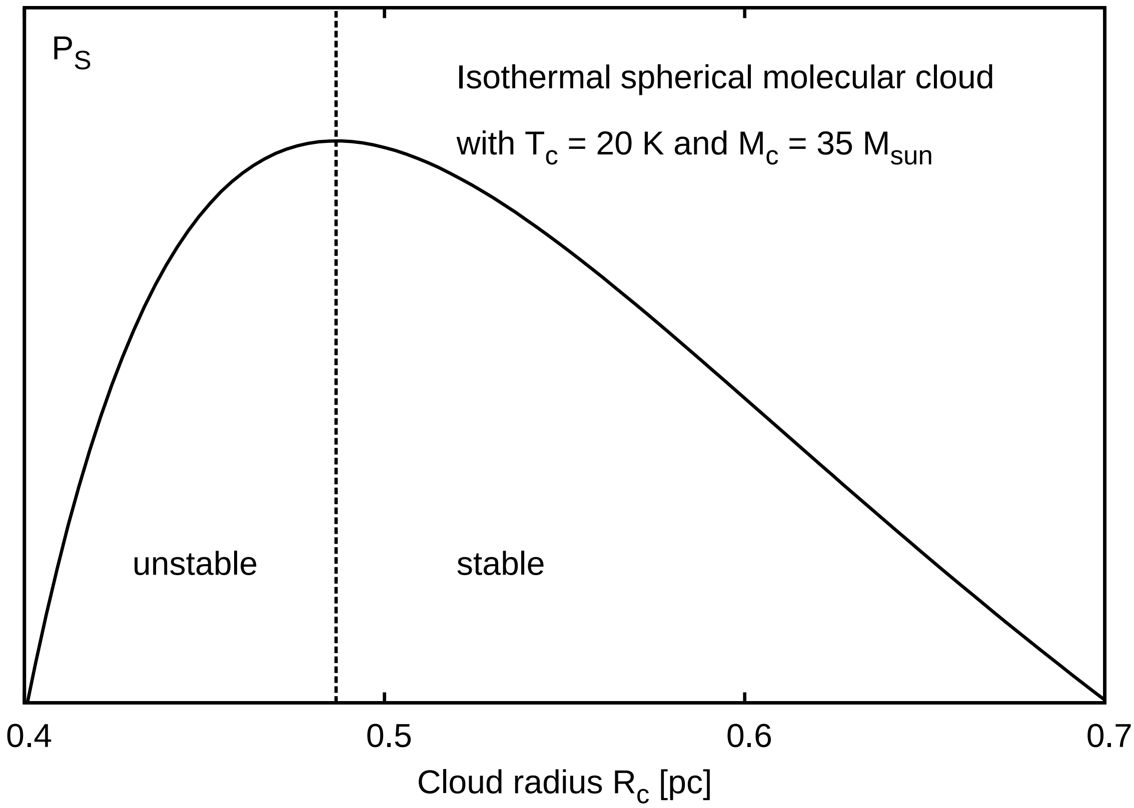

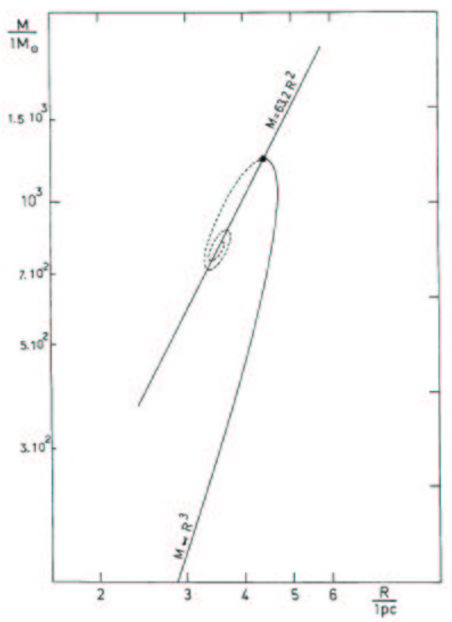

Fig. 1. The mass-radius relation for isothermal clouds with constant *surface* pressure ($T/\mu = 61.4$ K, $\bar{P}_0 = 3800$ K cm^{-3}). The critical point (•) separates the gravitationally stable configurations (solid line) from the unstable ones (dashed curve). This point moves on the straight line of slope 2 when the temperature is varied

Mass-radius relation for isothermal clouds with constant surface pressure (Chièze 1987)

- Sequential star formation
  - Cluster of stars forms within cloud
  - Winds from massive stars or supernova explosions cause shock waves and trigger star formation in other parts of the cloud

  → Chain of consecutive star formation episodes
  - Example: Scorpius-Centaurus association

Star formation history of the Scorpius-Centaurus association (Preibisch & Zinnecker 1999)

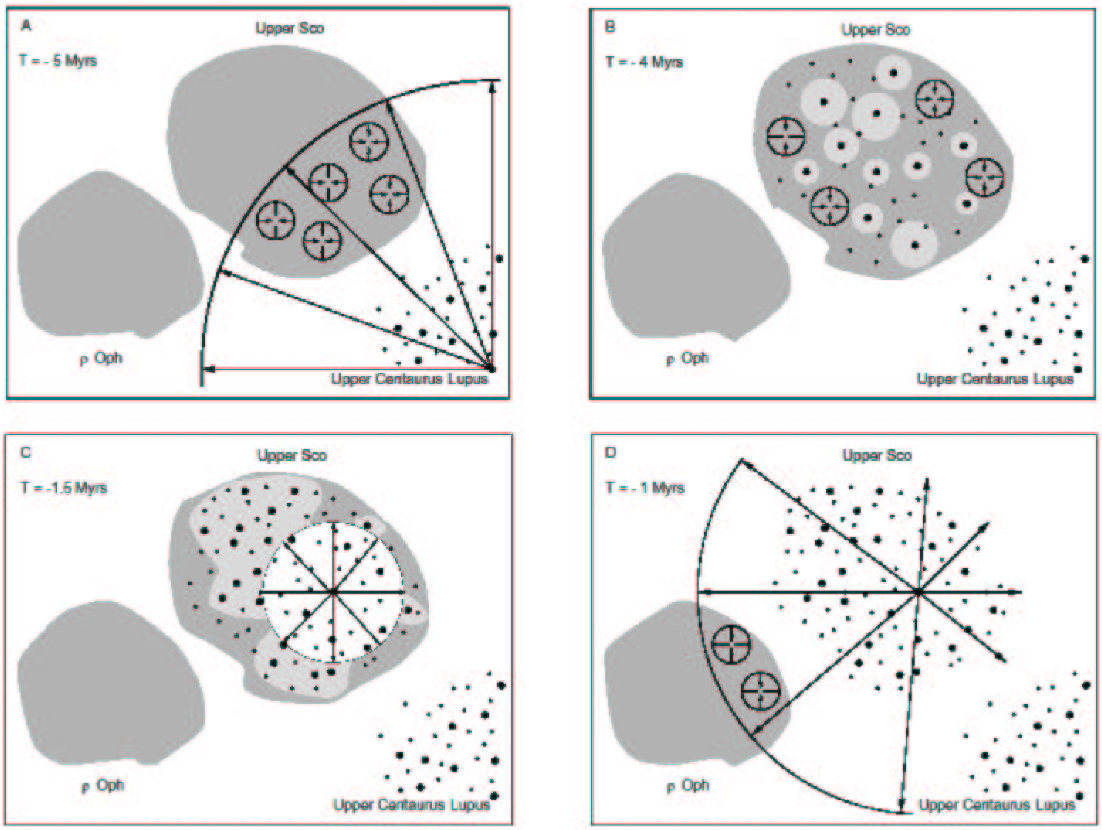

FIG. 8.—Schematic view of the star formation history in the Scorpius-Centaurus association. Molecular clouds are shown as dark regions, high-mass and low-mass stars as large and small dots, respectively. For further details on the sequence of events see § 9.2.

- Collapse calculations
  - Analytical and numerical studies of the collapse of an isothermal cloud
  - Determine the dynamical evolution of the system from solution of the equations for conservation of mass, equation of motion, and equation of state
  - Analytical self-similar solution for dependence of density on radius
    - fast increase of density towards the center
    - core with uniform density
    - matter falls onto core with ≈ free-fall velocity
    - shock forms at the edge of the core
    - outer layers fall slowly towards the center

Model for gravitational collapse (Blottiau et al. 1988)

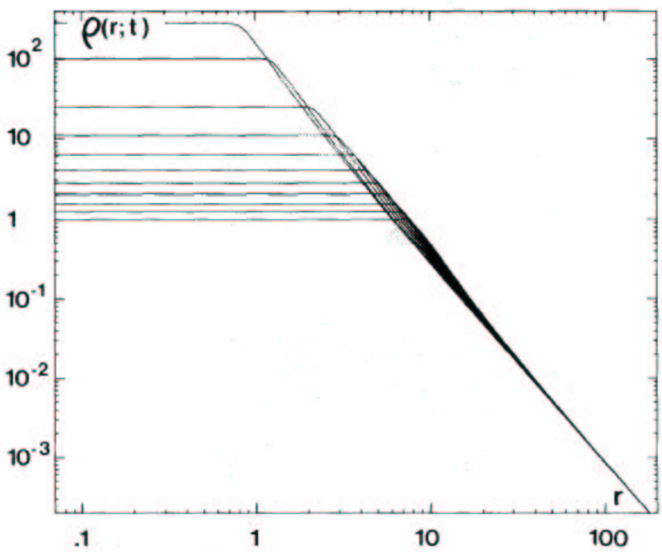

Fig. 3. $\boxed{\text{Analytical}}$ self-similar density profile $\rho(r;t)$ at different epochs for $\gamma = 1.20$. The units of density and radius are respectively $\rho(0,0)$ and $C_s(0,0)/|\Omega|$

Model for gravitational collapse (Blottiau et al. 1988)

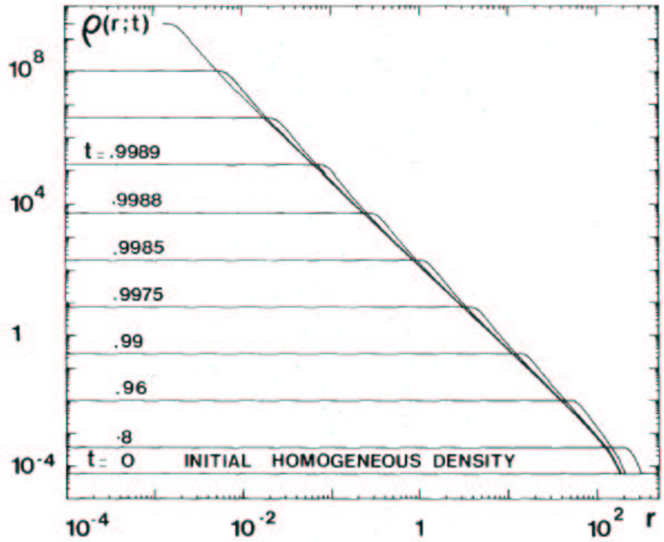

Fig. 7. Density profiles $\rho(r;t)$ at different epochs. These profiles result from the numerical evolution of a $\gamma = 1.20$ homogeneous gas cloud initially at rest.

- Major difficulties
  - Rotation
    - Angular momentum of collapsing cloud apparently not conserved
    - Efficient extraction of angular momentum must happen during formation process
  - Magnetic field
    - Influences star formation depending on field strength and coupling to gas
    - Magnetic field in stars much smaller than expected if ISM magnetic flux would remain frozen during star formation → decoupling must take place

Observations of star forming regions

- Infrared photometry:
  Young stellar objects show IR excesses because of dust disks
- Spectroscopy at mm wavelengths:
  lines from CO molecule → information on dynamics
- Example: RCW 108

4 F. Comerón, N. Schneider, and D. Russeil: Star formation in RCW 108

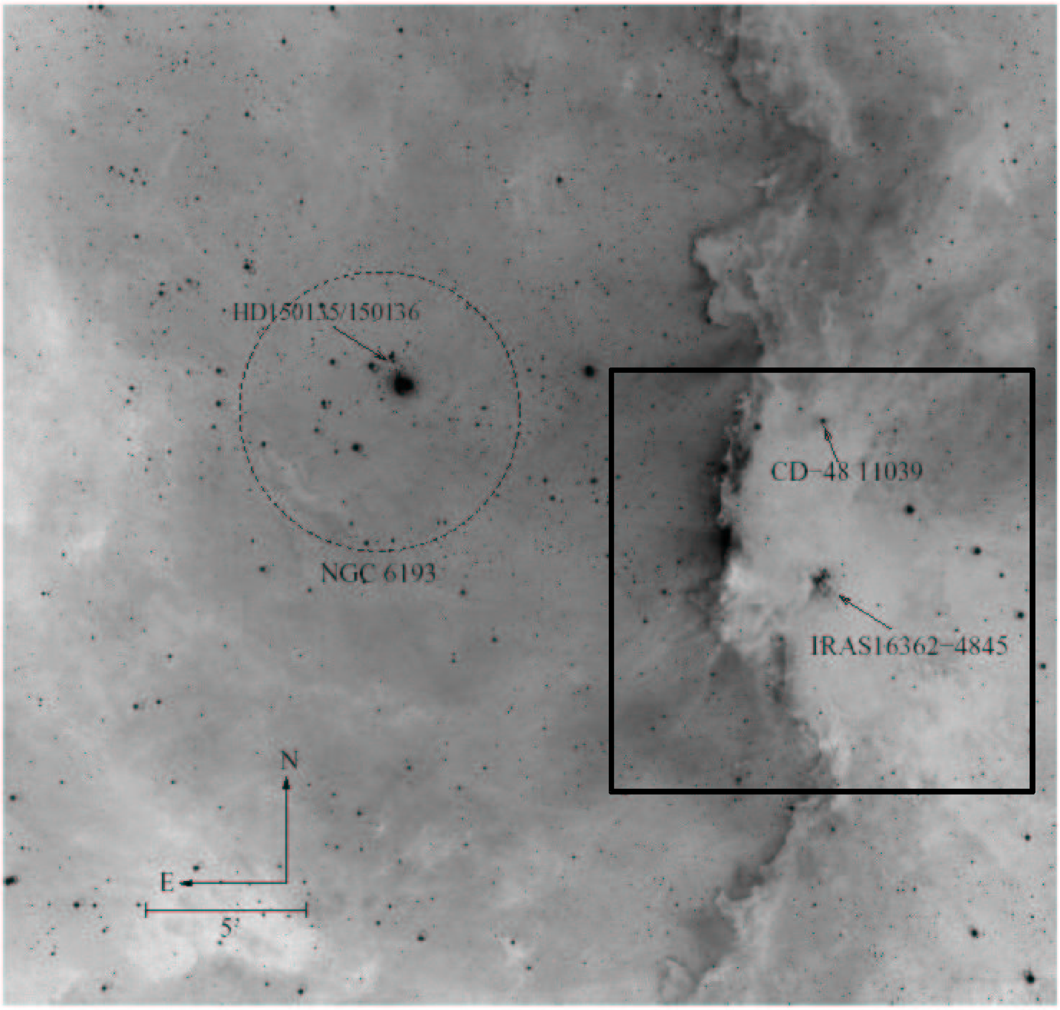

Fig. 1. A negative Hα wide-field image of the RCW 108 area (Sect. 2.4), showing the overall distribution of the ionized gas in the region and main objects discussed in the text. The large-scale distribution of the column density of obscuring dust can be inferred as well by noting the highly variable surface density of background stars across the field. The rings appearing around or next to bright stars are out-of-focus ghost images caused by internal reflections.

F. Comerón, N. Schneider, and D. Russeil: Star formation in RCW 108

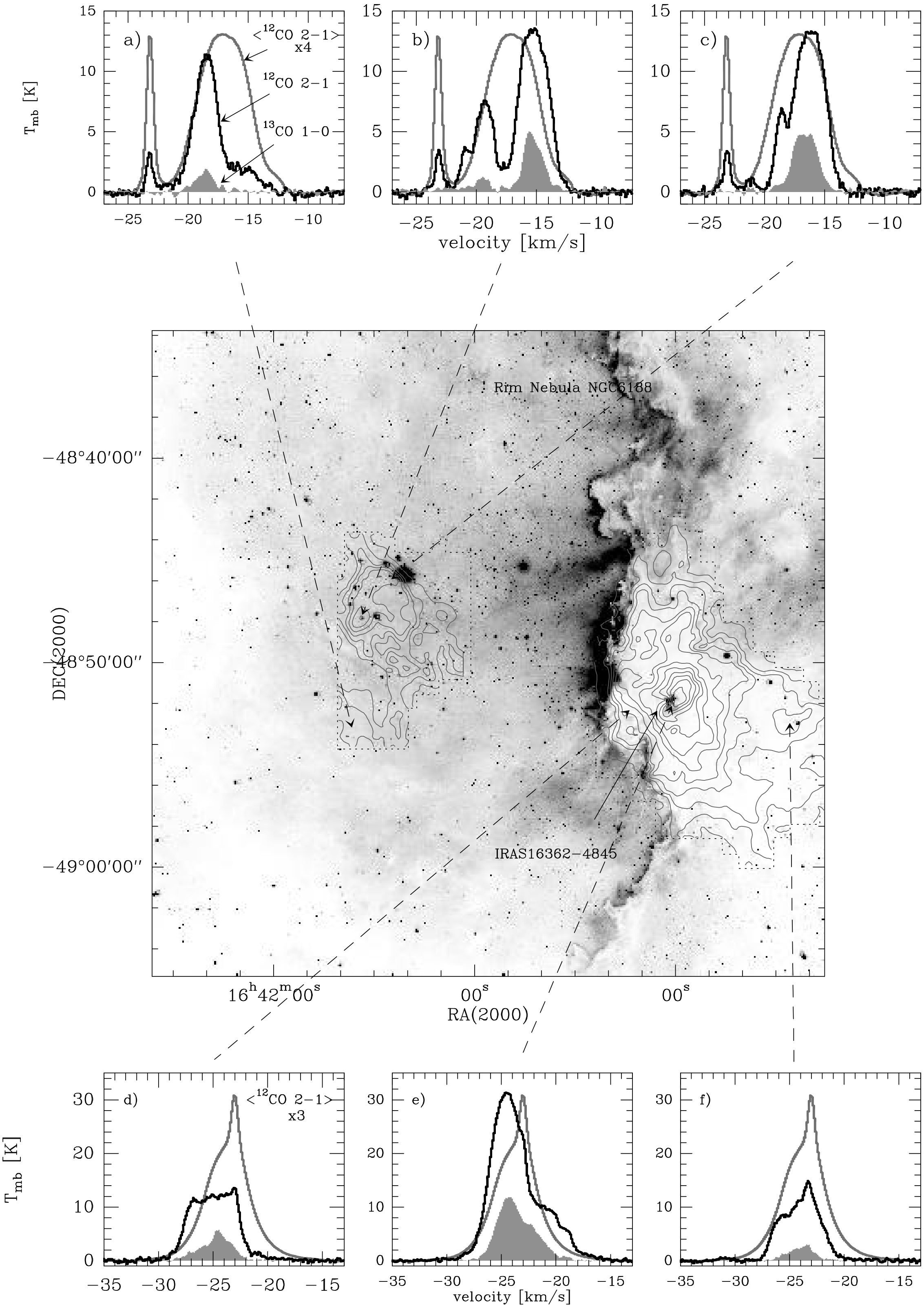

Comerón, Schneider & Russeil (astro-ph/0412125)

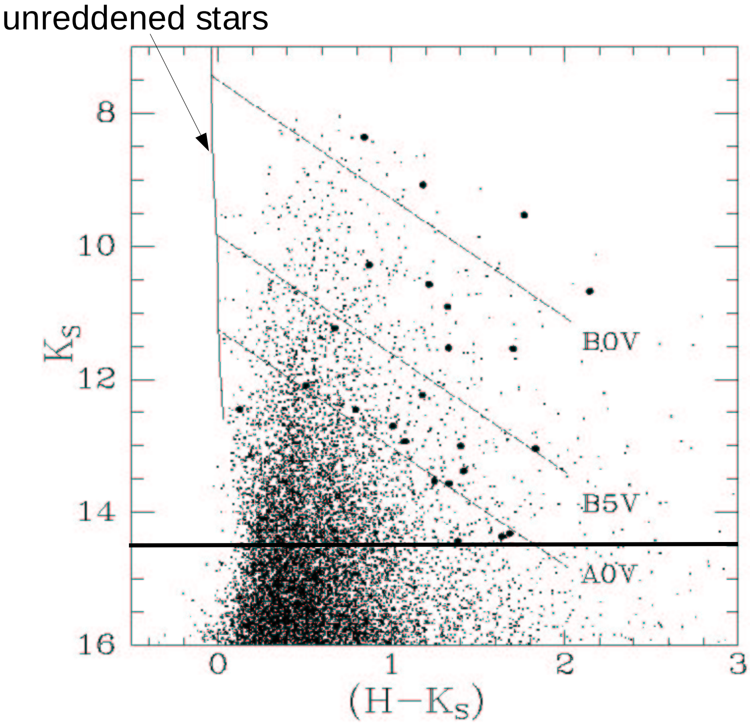

Near-infrared imaging of RCW 108:
J (1.25 μm)
H (1.65 μm)
K_s (2.2 μm)

range of $(H-K_S)$
$\rightarrow A_V = 8 \ldots 35$

Comerón, Schneider & Russeil (astro-ph/0412125)

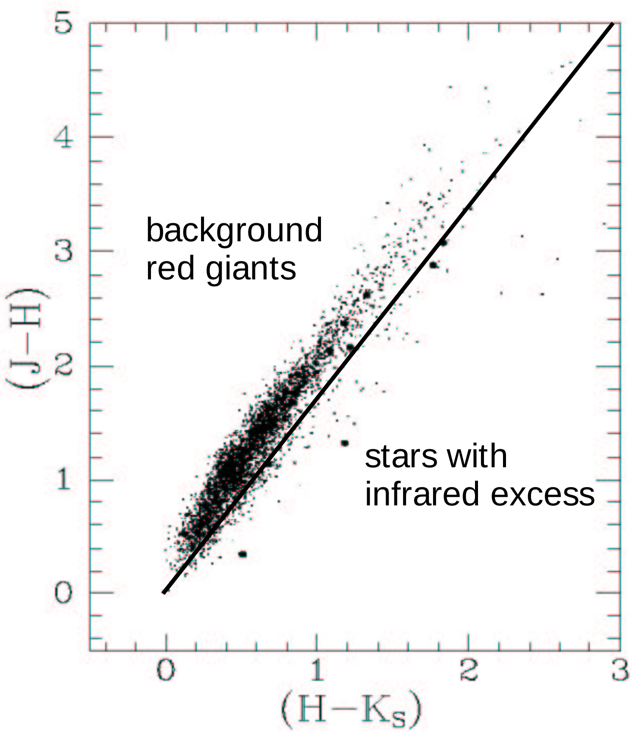

Stars brighter than K_s=14.5

Reddening vector for early type stars: $(J-H) = 1.7\ (H-K_s)$

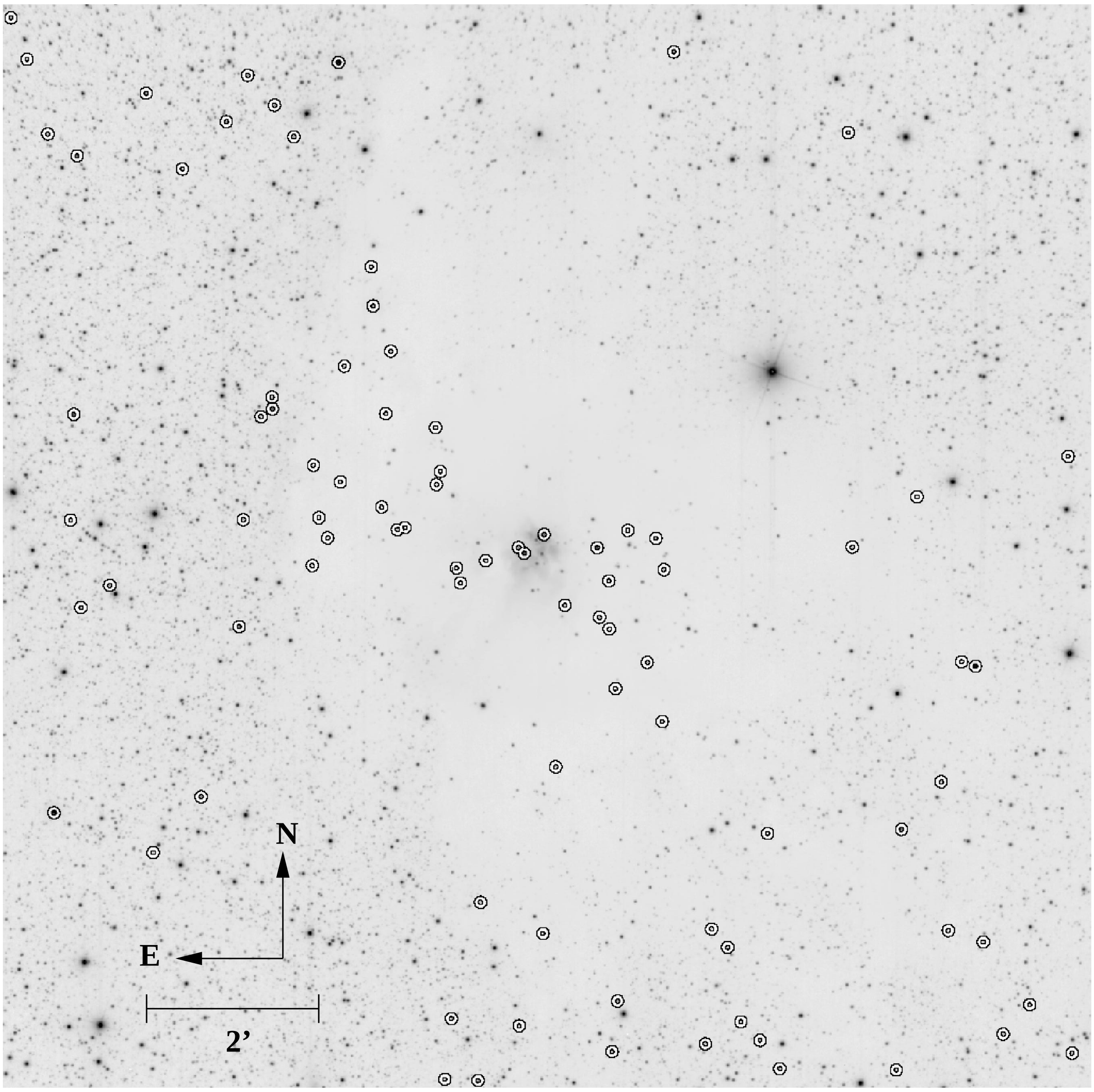

Fig. 20. K_S-band mosaic centered on the position of IRAS 16362-4845, containing most of the RCW 108 cloud and parts of its surrounding area. The circles mark the position of stars brighter than $K_S = 14.5$ displaying infrared excess emission according to the reddening-free Q parameter defined in Section 3.6.